J Ind Microbiol Biotechnol (2015) 42:1083–1089
DOI 10.1007/s10295-015-1626-5

SHORT COMMUNICATION

Stabilization of single species *Synechocystis* biofilms by cultivation under segmented flow

Christian David[1] · Katja Bühler[1] · Andreas Schmid[1]

Received: 16 February 2015 / Accepted: 25 April 2015 / Published online: 7 May 2015

Abstract The application of segmented flow on a *Synechocystis* sp. PCC 6803 biofilm prevented excessive biomass formation and clogging by fundamentally changing the structure of the microbial community. It was possible to continuously operate a capillary microreactor for 5 weeks, before the experiment was actively terminated. The biofilm developed up to a thickness of 70–120 µm. Surprisingly, the biofilm stopped growing at this thickness and stayed constant without any detachment events occurring afterwards. The substrates CO_2 and light were supplied in a counter-current fashion. Confocal microscopy revealed a throughout photosynthetically active biofilm, indicated by the red fluorescence of photo pigments. This control concept and biofilm reaction setup may enable continuous light driven synthesis of value added compounds in future.

Keywords Cyanobacteria · Biofilm · Hydrodynamic · Continuous bioprocess · Photosynthesis

Introduction

Biofilms are cellular communities attached to surfaces and embedded in self-produced extracellular polymeric substances (EPS). In the broadest sense, all kinds of microbial structures like cell aggregates (flocs), sedimented layers or tightly attached films can be defined as biofilms [1, 2]. They are omnipresent in nature, where they are often found as multispecies microbial mats. In such structures, a complex system of interrelated dependencies of various organisms comprising phototrophic and heterotrophic strains exists. Biofilms are also very important in artificial medical or technical settings, although there they are mostly unwanted, as biofilms are very persistent and lead to biofouling or severe infections. However, these characteristics could be beneficial in terms of process stability and a continuous process mode for biocatalysis and the production of value added compounds with biologically challenging reactants as shown recently [3]. Higher overall robustness, self-regeneration and immobilization with high biomass retention are main characteristics for catalytically active biofilms [4, 5]. Key challenges when applying catalytic biofilms in continuous processes include mass transfer through the three-dimensional structures of cells and EPS substances and excessive biomass formation resulting in clogging. One approach to circumvent these bottlenecks is the formation of a flat, compact film. This can be achieved by cultivating the respective microbes in capillary tubings under continuous flow applying hydrodynamic forces. These may be generated by two-phase segmented flow, consisting of an aqueous and a gaseous phase [6]. The heterotrophic model strain used in this study, *Pseudomonas taiwanensis* VLB120, had to adapt over several days to the high interfacial forces, and formed a completely different structure under segmented as compared to single phase flow. This was highly beneficial for the respective biotransformation rates and provided a basis for a truly continuous process format. While applications of heterotrophic biofilms are well described, examples using photoautotrophic organisms as biofilm catalysts are missing up to date, although numerous studies reported proves of concept for the synthesis of value added compounds by suspended phototrophic organisms like cyanobacteria and/or microalgae [7–13].

✉ Katja Bühler
katja.buehler@ufz.de

[1] Department Solar Materials, Helmholtz Centre for Environmental Research (UFZ), Permoserstraße 15, 04318 Leipzig, Germany

In ecology, natural phototrophic-heterotrophic multispecies biofilm communities play a major role for ecosystem assessment and are frequently studied [14–19], whereas studies of phototrophic biofilms for synthetic and technical applications are limited [20]. Examples include microbial fuel cells [21] and applications in waste water treatment [22]. While in waste water treatment huge amounts of biomass are generated, microbial fuels cells represent a static non-flow system without hydrodynamic forces. Such systems are not suited for applications in whole cell biocatalysis due to mass transfer limitations and uncontrolled biomass growth [23]. The development of suitable cultivation concepts and the identification and characterization of monospecies biofilms will be essential for applications of phototrophic biofilms as catalysts in synthetic chemical industries.

We present growth controlled cultivation applying a segmented type of flow and the initial characterization of a monospecies *Synechocystis* sp. PCC 6803 biofilm in a micro capillary flow through reactor. Significant differences in biofilm growth could be observed depending on the hydrodynamic conditions applied. While under single phase flow, clogging of the capillary occurred due to uncontrolled biomass formation, a photosynthetically active, flat and compact biofilm structure was formed upon the introduction of air segment into the system without any cell detachment events.

In future combinations with metabolic engineering of *Synechocystis* sp. PCC 6803, this biofilm reaction setup may enable continuous light driven syntheses of value added compounds.

Materials and methods

Chemicals and bacterial strains

All chemicals used were obtained from AppliChem (Darmstadt, Germany), Sigma Aldrich (Steinheim, Germany), or CarlRoth (Karlsruhe, Germany) with the highest purity available. The cyanobacterial strains *Synechocystis* sp. PCC 6803 [24] and *Synechococcus elongatus* PCC 7942 [25] were obtained from the Pasteur Culture Collection of Cyanobacteria (PCC, Paris, France).

Cultivation of cyanobacterial strains

Precultures for biofilm inoculation were grown in 50 mL baffled shaking flasks in a Multitron shaker (Infors, Bottmingen, Switzerland), equipped with light tubes (Osram Lumilux L18 W/840 cool white) and humidity control. 10 mL of YBG11 medium [26] was inoculated from a cryo stock and strains were cultivated at 30 °C, 150 rpm, 80 % relative humidity and 50 µE m^{-2} s^{-1} photosynthetically active radiation (PAR). For long-term storage the strains were frozen in YBG11 medium containing 8 % DMSO at −80 °C.

Experimental biofilm setup

Biofilms were cultivated in rectangular-shaped borosilicate glass capillaries (Fig. 1) suitable for CLSM investigation [6]. YBG11 medium was supplied through Tygon Standard R-3607 tubing (2.06 mm inner diameter, Ismatec, Wertheim-Mondfeld, Germany) by a peristaltic pump (ISM 930; Ismatec, Wertheim-Mondfeld, Germany). In case of segmented flow, additional tubing was connected via a T-connector and a sterile filter (0.2 µm) for the introduction of air segments. The assembled flow cell was heat sterilized. Afterwards the system was flushed with YBG11 and adjusted to 30 °C and 55 µE m^{-2} s^{-1}. If not stated otherwise, the biofilm flow cells were inoculated with cells in 800 µL of preculture with an OD_{750} of 1.0. Cell attachment occurred in 24 h without flow. Subsequently, the medium flow was started. Two different flow patterns and their influence on biofilm development have been evaluated—*single phase flow:* After the cell attachment phase the flow was set to 100 µL min^{-1} (1.4 cm min^{-1}) unless indicated

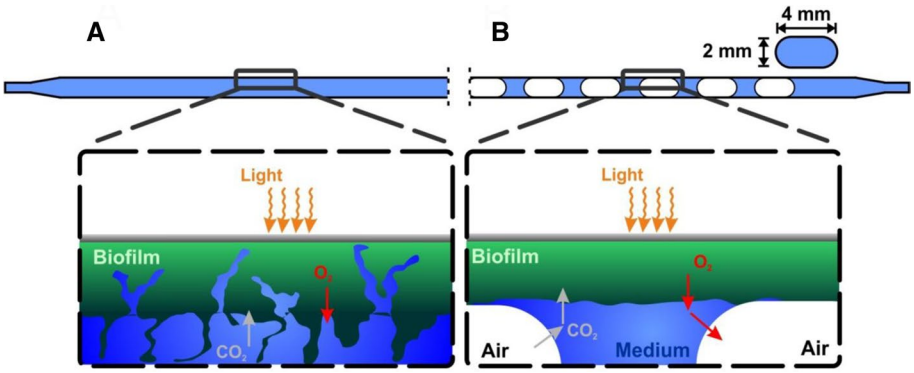

Fig. 1 Schematic representation of the biofilm reactor (capillary length 80 mm) operated in single phase flow (**a**) and segmented flow mode (**b**). Light is absorbed and scattered on its way through the individual biofilm layers, whereas CO_2 is consumed by the cells resulting in a CO_2 gradient. O_2 produced by photosynthesis is leaving the system via the bulk phase

otherwise. The flow was kept constant during the whole cultivation time; *segmented flow:* After the cell attachment phase the flow was set to 100 µL min^{-1} (1.4 cm min^{-1}) and kept constant for 2 days. Subsequently segmented flow was established and air segments were introduced into the aqueous phase at 50 µL min^{-1} while the aqueous flow was reduced to 50 µL min^{-1}, resulting again in an overall flow rate of 100 µL min^{-1} (1.4 cm min^{-1}). For more details, please see text. An overview showing the reactor system is presented in Fig. 1.

Analytical procedures

Planktonic cell growth was quantified by turbidity measurements (OD_{750}, Libra S11, Biochrom Ltd, Cambridge, UK). Photosynthetically active radiation (PAR) was determined with a MQS-B mini quantum sensor coupled to an ULM-500 light meter (Heinz Walz GmbH, Effeltrich, Germany).

Biofilm development on the glass surface was monitored in situ using a Zeiss LSM 5 Pascal confocal laser-scanning microscope (CLSM; Carl Zeiss, Jena, Germany), equipped with an argon and helium–neon laser and an EC Plan-Neofluar 20x, 0.50 Ph2 M27 objective, taking advantage of the natural autofluorescence of chlorophyll and the phycobilins phycocyanin, allophycocyanin and allophycocyanin-B [27, 28]. For photosynthetically non-active cells, the autofluorescence of carotenoids was detected as described earlier [28, 29]. Three-dimensional (3D) biofilm image reconstructions were performed by IMARIS (Bitplane AG, Zürich, Switzerland).

Results and discussion

Robust biofilm formation with *Synechocystis* sp. PCC 6803

For the investigation of biofilm formation, flow cells were inoculated with *Synechococcus elongatus* PCC 7942 and *Synechocystis* sp. PCC 6803, respectively. Under the conditions applied, *Synechococcus elongatus* PCC 7942 did not attach to the glass substratum. A reason why cell attachment and biofilm formation with this strain was not possible may be a mechanism for self-suppression of biofilm formation induced by a self-produced extracellular compound, as reported recently [30]. In contrast to that, initial cell attachment of *Synechocystis* sp. PCC 6803 to the glass surface of the flow cell reactor took place within 4 h. Since *Synechocystis* sp. PCC 6803 showed strong biofilm formation, biofilm growth and morphology were characterized under different hydrodynamic conditions.

Uncontrolled heterogeneous single species biofilm formation under single phase flow

No-flow, batch incubations in the tube allowed sufficient initial cell attachment overnight. Then, at an applied flow rate of 50 µL min^{-1} (0.7 cm min^{-1}), exponential growth was observed during the first 72 h of the experiment at a growth rate of 0.045 h^{-1}, calculated based on the increase in overall biofilm volume. A gradient in biofilm thickness toward a thinner film at the outflow was observed over the reactor length. Most probably this was due to carbon dioxide depletion at this low flow rate. *Synechocystis* sp. PCC 6803 formed a very heterogeneous biofilm under these conditions without an area-wide sublayer and with a porous structure interconnected by channels and elongated streamers. Overall, this resulted in a high surface ratio of 5.5 μm^2 μm^{-2}, and an inhomogeneous thickness and light distribution (Fig. 2a). After 7 days the flow rate was increased to 100 µL min^{-1} (1.4 cm min^{-1}), preventing CO_2 limitation. To exclude an influence of the carbon dioxide limitation in the beginning of the experiment on the overall development of the biofilm structure, we repeated the experiment with an initial flux of 100 µL min^{-1} (1.4 cm min^{-1}). The same heterogeneous biofilm structure described before was observed.

After 14 days of constant flow, the capillary started to clog and as a result the system pressure increased and a constant flow was not possible anymore. At this time point the biofilm was in large parts still permeable to light, but could not be supplied with CO_2 any longer.

Segmented flow shapes and stabilizes single species biofilm development

The capillary plug flow reactor was inoculated with *Synechocystis* sp. PCC 6803. After initial overnight cell attachment under batch conditions (non-continuous) and 2 days of single phase flow (100 µL min^{-1}, 1.4 cm min^{-1}), air segments were introduced as described in the method section. The air segments generated interfacial forces between 1.36×10^{-7} and 1.36×10^{-6} N (calculated according to [6]), in addition to a better availability of the substrate CO_2. Surprisingly, this did not result in a significant detachment processes as observed for *Pseudomonas* under segmented flow [6]. In fact, no wash out of cells could be detected throughout the experiment. The attachment forces of the cells to the substratum are possibly much higher for *Synechocystis* sp. PCC 6803 compared to the heterotrophic Pseudomonas strain reported earlier. There, the interfacial forces generated by the segmented type of flow were strong enough to nearly completely detach all cells from their growth surface [6]. For *Synechocystis* a growth rate

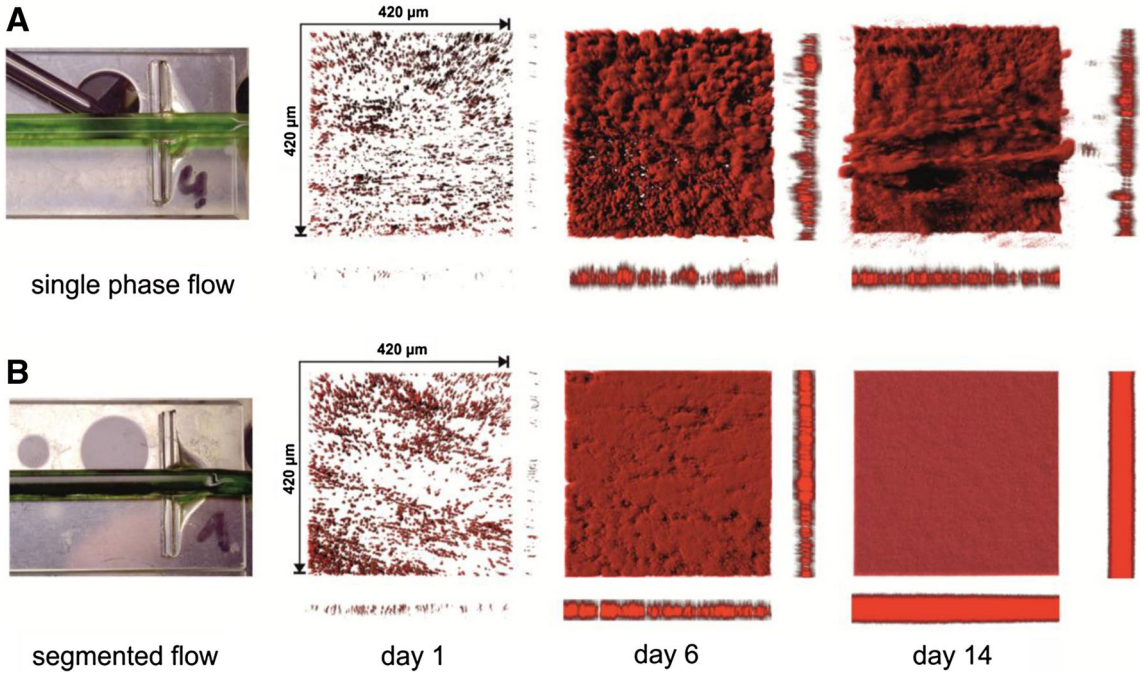

Fig. 2 Representative images showing the differences in development of *Synechocystis* sp. PCC 6803 biofilms grown under single phase flow (**a**) and segmented flow (**b**). The first picture in every row shows a photo of the fully grown biofilm inside the glass capillary reactor. The following illustrations are 3D-reconstructions of the biofilm generated from CLSM data by IMARIS. The *top* views on the biofilm surface as well as cross sections of the biofilm are included. The first pictures were taken directly after starting the flow. In case of segmented flow the biofilm thickness at day 6 and 14 exceeds already the penetration capacity of the applied LSM technique

of 0.045 h^{-1} was determined during the first 72 h, which is comparable to the growth rates without segmented flow described above. However, segmented flow changed the biofilm structure dramatically. If the CO_2 availability had any impact regarding the change in biofilm structure remains to be elucidated. There are no indications for a CO_2 limitation in either system [single (100 µL min^{-1})/two-phase flow], as for both equal biofilm thicknesses from the beginning to the end of the plug flow reactor were determined, pointing toward a sufficient supply of this substrate.

During the first 14 days of the experiment, a homogenous, dense biofilm layer developed (Fig. 2b). The autofluorescence intensity, used for quantification of biomass development, is significantly higher compared to the biofilm grown under single phase flow. The signal intensity determined from the biofilm was depending on cell density and pigment concentration within the cells. Especially the latter is subject to changes due to adaptation to different light conditions and is influenced by laser irradiation of the CLSM. Nevertheless, this signal may be used for a qualitative assessment of the biofilm biomass.

At some point of growth, the biofilm thickness and the density of the mature biofilm grown under segmented flow exceeded the penetration capacity of the CLSM system and the biofilm thickness could no longer be determined (Fig. 2b). Yet, it was possible to characterize the further development of the biofilm by eye. Within 3 weeks, the biofilm grown in the capillary appeared nearly black. In contrast to the non-segmented aqueous microreactor described above, the biofilm reactor could be continuously operated for 5 weeks before it was actively terminated. Neither was there an indication that the biomass increased further during this time period, nor were any cells detectable in the flow through. Phototrophic segmented flow capillary biofilm reactors are therefore powerful tools to control and even prevent excess biomass formation and to keep the process controllable.

Key parameters affecting *Synechocystis* sp. PCC 6803 biofilm development

Key parameters for biocatalytic and biotechnological applications of cyanobacterial biofilms are the distribution of light and the diffusional limitation of carbon dioxide within the biofilm. In case of heterotrophic biofilms, the efficient supply of nutrients is a matter of diffusion, in most cases directly from the aqueous bulk phase. In contrast, light availability, essential for the growth of phototrophic biofilms, is determined via light scattering within the biofilm.

In natural phototrophic-heterotrophic mixed species biofilm communities, the special distribution of photo- and heterotrophic organisms, the attenuation of light intensity

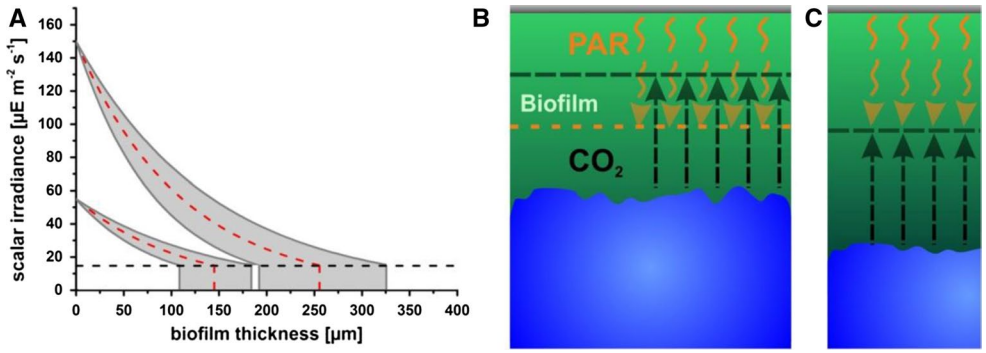

Fig. 3 **a** Exponential light attenuation within a cyanobacterial biofilm calculated from data published for an artificial cyanobacterial mat [17]. The *gray areas* represent the estimated light attenuation for incidental light intensities of 55 and 150 µE m^{-2} s^{-1} with a light attenuation coefficient between 7 and 12 mm^{-1} (*right* and *left* borders, respectively). Additionally the results for an attenuation coefficient of 9 mm^{-1} are highlighted (**- - -**). *Horizontal line* represents the boundary of 15 µE m^{-2} s^{-1} where growth of *Synechocystis* sp. PCC 6803 is significantly decreased. **b**, **c** Schematic distribution of the main substrates carbon dioxide and photosynthetically active radiation (PAR) within the biofilm and the resulting potential growth zones

and the photosynthesis rate within these microbial mats have been intensively investigated [14–16, 31]. Depending on the densities of the investigated mats specific light attenuation coefficients were reported, which gave a basis for estimating respective values for the here cultivated *Synechocystis* biofilms (Fig. 3). Related to the observed structure of the biofilm growing in the microcapillaries, light attenuation coefficients between 7 and 12 mm^{-1} were estimated.

The light attenuation coefficient together with the intensity of the available incident light defines the borders of growth in three-dimensional structures as biofilms. For the cyanobacterium *Oscillatoria agardhii* these limits have been closely evaluated. Below 20 µE m^{-2} s^{-1} a significant decrease in the growth rate was observed, while above 150 µE m^{-2} s^{-1} light inhibition occurred [32]. Based on these values a maximal thickness for *Synechocystis* biofilms cultivated under the herein described conditions has been calculated. Assuming the maximal possible light intensity of 150 µE m^{-2} s^{-1} and a light attenuation coefficient of 9 mm^{-1}, which can be assumed for a biofilm grown under single phase flow conditions, a maximal biofilm thickness of 250 µm can be theoretically achieved. The maximal biofilm thickness to be expected under our experimental conditions (55 µE m^{-2} s^{-1}) during single phase flow was about 150 µm (Fig. 3a). The light attenuation coefficient under segmented flow is significantly higher because of higher cell densities. With a theoretical light attenuation coefficient of 12 mm^{-1}, the expected biofilm thickness would be around 105 µm, which is far beyond the detection limit of the available CLSM system. Therefore, after 5 weeks of segmented flow biofilm development, cross sections have been prepared from the capillary and were investigated by CLSM. This allowed the determination of a final maximal biofilm thickness between 70 and 120 µm. Biofilms are heterogenic, dynamic, three-dimensional structures comprising areas with high cell densities, low cell densities, and channels without any cells. These differences in the composition strongly influence the light attenuation in the biofilm and thus the possible biofilm thickness. Interestingly, the biofilm cross sections were made up nearly exclusively of photosynthetically active cells and only a few cells (<1 %) without photopigments could be localized, homogenously distributed throughout the biofilm. The anticipated limit for light availability lies within the measured range. Also important, the observed differences in biofilm thickness are corresponding to the expected variances in light attenuation within the biofilm. The negligible biomass concentration in the outlet stream, in addition to the fact, that there were nearly no photosynthetically inactive cells detected at the inner-tube biofilm surface led to the conclusion that there is no significant biomass formation within the reactor anymore. Theoretically, one would expect biofilm growth up to a thickness, where one of its main substrates, carbon dioxide or light, becomes limiting. Thus, maximal light and carbon dioxide penetration depth would define the borders of biofilm growth (Fig. 3b). This opens the question why further growth was not observed in our experiments. One explanation might be a quorum sensing signal, which prevents growth within the center of the biofilm, in the presence of high cell density [33]. Additionally, the oxygen produced within the biofilm might also be a reason for limited growth. A high oxygen concentration would have a negative impact on the carbon capture ability of the cells [34].

Reactor and process engineering for phototrophic whole cell biocatalysis require a rethinking of common reactor concepts. The essential substrates light, water, and carbon dioxide necessitate different process concepts and technical solutions compared to today´s applications in biotechnology. The available reactor configurations aim at maximal

biomass production; however, this is usually suboptimal. This is also true for the suitability of biofilms as catalysts for continuous chemical synthesis which necessitates controllable porosity and growth as well as activity of all cells in the biofilms. For phototrophic microorganisms these qualities are for the first time met for the concept described herein. In our opinion, continuous processes, controlled biomass formation and regeneration of the biocatalyst are mandatory to enable the efficient production of value added compounds and biofuels from sunlight and CO_2.

Concluding remarks

Biofilms are important functional modules in many synthetic bioprocesses. Their productivity is determined by stability, morphology, and control of biofilm development and growth. This report communicates a new methodology for developing, cultivating, and controlling a monospecies cyanobacterial biofilm of *Synechocystis* sp. PCC 6803 using a microcapillary reactor with continuous segmented flow. This concept provides a unique possibility to control biofilm growth and is a potent technology for the application of phototrophic cyanobacterial biofilms. This provides a basis for future investigations of biofilm growth and production characteristics also of other cyanobacterial strains. Open questions include scalability, molecular regulation influencing biofilm formation and solvent tolerance.

Acknowledgments We are grateful to Carl Zeiss Microscopy, especially Dr. F. Josten for technical and apparative support, to the Chair of Chemical Biotechnology (TU Dortmund) for lab space and support, and to Dr. B. Halan and Dr. R. Karande for the helpful discussions.

Conflict of interest The authors declare no commercial or financial conflict of interest.

References

1. Flemming H-C, Wingender J (2010) The biofilm matrix. Nat Rev Microbiol 8:623–633. doi:10.1080/0892701031000072190
2. Wingender J, Neu TR, Flemming H-C (1999) Microbial extracellular polymeric substances. Springer, Berlin Heidelberg, pp 1–19
3. Gross R, Buehler K, Schmid A (2013) Engineered catalytic biofilms for continuous large scale production of n-octanol and (*S*)-styrene oxide. Biotechnol Bioeng 110:424–436. doi:10.1002/bit.24629
4. Halan B, Buehler K, Schmid A (2012) Biofilms as living catalysts in continuous chemical syntheses. Trends Biotechnol 30:453–465. doi:10.1016/j.tibtech.2012.05.003
5. Rosche B, Li XZ, Hauer B et al (2009) Microbial biofilms: a concept for industrial catalysis? Trends Biotechnol 27:636–643. doi:10.1016/j.tibtech.2009.08.001
6. Karande R, Halan B, Schmid A, Buehler K (2014) Segmented flow is controlling growth of catalytic biofilms in continuous multiphase microreactors. Biotechnol Bioeng 111:1831–1840. doi:10.1002/bit.25256
7. Ducat DC, Way JC, Silver PA (2011) Engineering cyanobacteria to generate high-value products. Trends Biotechnol 29:95–103. doi:10.1016/j.tibtech.2010.12.003
8. Ruffing AM (2011) Engineered cyanobacteria: teaching an old bug new tricks. Bioeng Bugs 2:136–149. doi:10.4161/bbug.2.3.15285
9. Wijffels RH, Kruse O, Hellingwerf KJ (2013) Potential of industrial biotechnology with cyanobacteria and eukaryotic microalgae. Curr Opin Biotechnol 24:405–413. doi:10.1016/j.copbio.2013.04.004
10. Gudmundsson S, Nogales J (2015) Cyanobacteria as photosynthetic biocatalysts: a systems biology perspective. Mol BioSyst 11:60–70. doi:10.1039/c4mb00335g
11. Nogales J, Gudmundsson S, Thiele I (2013) Toward systems metabolic engineering in cyanobacteria. Bioengineered 4:158–163. doi:10.4161/bioe.22792
12. Angermayr SA, Hellingwerf KJ, Lindblad P, de Mattos MJT (2009) Energy biotechnology with cyanobacteria. Curr Opin Biotechnol 20:257–263. doi:10.1016/j.copbio.2009.05.011
13. Abed RMM, Dobretsov S, Sudesh K (2009) Applications of cyanobacteria in biotechnology. J Appl Microbiol 106:1–12. doi:10.1111/j.1365-2672.2008.03918.x
14. Kühl M, Fenchel T (2000) Bio-optical characteristics and the vertical distribution of photosynthetic pigments and photosynthesis in an artificial cyanobacterial mat. Microb Ecol. doi:10.1007/s002480000061
15. Fenchel T, Kühl M (2000) Artificial cyanobacterial mats: growth, structure, and vertical zonation patterns. Microb Ecol 40:85–93. doi:10.1007/s002480000062
16. Al-Najjar MAA, de Beer D, Kühl M, Polerecky L (2012) Light utilization efficiency in photosynthetic microbial mats. Environ Microbiol 14:982–992. doi:10.1111/j.1462-2920.2011.02676.x
17. Zippel B, Neu TR (2005) Growth and structure of phototrophic biofilms under controlled light conditions. Water Sci Technol 52:203–209
18. Zippel B, Rijstenbil J, Neu TR (2007) A flow-lane incubator for studying freshwater and marine phototrophic biofilms. J Microbiol Methods 70:336–345. doi:10.1016/j.mimet.2007.05.013
19. Wolf G, Picioreanu C, van Loosdrecht MCM (2007) Kinetic modeling of phototrophic biofilms: the PHOBIA model. Biotechnol Bioeng 97:1064–1079. doi:10.1002/bit.21306
20. Fresewinkel M, Rosello R, Wilhelm C et al (2014) Integration in microalgal bioprocess development: design of efficient, sustainable, and economic processes. Eng Life Sci. doi:10.1002/elsc.201300153
21. McCormick AJ, Bombelli P, Scott AM et al (2011) Photosynthetic biofilms in pure culture harness solar energy in a mediatorless bio-photovoltaic cell (BPV) system. Energy Environ Sci 4:4699. doi:10.1039/c1ee01965a
22. Roeselers G, Van Loosdrecht MCM, Muyzer G (2008) Phototrophic biofilms and their potential applications. J Appl Phycol 20:227–235. doi:10.1007/s10811-007-9223-2
23. Van Loosdrecht MCM, Heijnen S (1993) Biofilm bioreactors for waste-water treatment. Trends Biotechnol 11:117–121. doi:10.1016/0167-7799(93)90085-N
24. Stanier RY, Kunisawa R, Mandel M, Cohen-Bazire G (1971) Purification and properties of unicellular blue-green algae (Order *Chroococcales*). Bacteriol Rev 35:171–205
25. Rippka R, Deruelles J, Waterbury JB et al (1979) Generic assignments, strain histories and properties of pure cultures of cyanobacteria. J Gen Microbiol 111:1–61
26. Shcolnick S, Shaked Y, Keren N (2007) A role for mrgA, a DPS family protein, in the internal transport of Fe in the cyanobacterium *Synechocystis* sp. PCC 6803. Biochim Biophys Acta 1767:814–819. doi:10.1016/j.bbabio.2006.11.015

27. Mariné MH, Clavero E, Roldán M (2004) Microscopy methods applied to research on cyanobacteria. Limnetica 23:179–186
28. Vermaas WFJ, Timlin JA, Jones HDT et al (2008) In vivo hyperspectral confocal fluorescence imaging to determine pigment localization and distribution in cyanobacterial cells. Proc Natl Acad Sci USA 105:4050–4055. doi:10.1073/pnas.0708090105
29. Schulze K, López DA, Tillich UM, Frohme M (2011) A simple viability analysis for unicellular cyanobacteria using a new autofluorescence assay, automated microscopy, and ImageJ. BMC Biotechnol 11:118. doi:10.1186/1472-6750-11-118
30. Schatz D, Nagar E, Sendersky E et al (2013) Self-suppresion of biofilm formation in the cyanobacterium *Synechococcus elongatus*. Environ Microbiol 15:1786–1794. doi:10.1111/1462-2920.12070
31. Kühl M, Glud RRN, Ploug H, Ramsing NNB (1996) Microenvironmental control of photosynthesis and photosynthesis-coupled respiration in an epilithic cyanobacterial biofilm. J Phycol 32:799–812. doi:10.1111/j.0022-3646.1996.00799.x
32. Tilzer MM (1987) Light-dependence of photosynthesis and growth in cyanobacteria: implications for their dominance in eutrophic lakes. New Zeal J Mar Freshw Res 21:401–412. doi:10.1080/00288330.1987.9516236
33. Ng W-L, Bassler BL (2009) Bacterial quorum-sensing network architectures. Annu Rev Genet 43:197–222. doi:10.1146/annurev-genet-102108-134304
34. Daley SME, Kappell AD, Carrick MJ, Burnap RL (2012) Regulation of the cyanobacterial CO_2-concentrating mechanism involves internal sensing of $NADP^+$ and α-ketogutarate levels by transcription factor CcmR. PLoS One 7:e41286. doi:10.1371/journal.pone.0041286